Supporting Information

Photochromic and Electrochromic Properties of Viologen-Based Multifunctional Cd-MOF

Hai-Yang Li,[a†] Xue Hua,[a†] Ting Fu,[a] Xiao-Fei Liu*[a] and Shuang-Quan Zang*[a]

[a] *Henan Key Laboratory of Crystalline Molecular Functional Materials, Henan International Joint Laboratory of Tumor Theranostical Cluster Materials, Green Catalysis Center, and College of Chemistry, Zhengzhou University, Zhengzhou 450001, China*

[†] *These authors contributed equally to this work.*

E-mail: zangsqzg@zzu.edu.cn; liuxiaofei@zzu.edu.cn

Experimental Section

Reagents and Materials

All solvents and chemicals, including cadmium chloride hemipentahydrate ($CdCl_2 \cdot 5/2H_2O$), dimethylacetamide (DMAc), D/L-tartaric acid, were commercially available and were not require further processing. 1-(3,5-dicarboxybenzyl)-4,4′-bipyridinium chloride ($H_2L^+ \cdot Cl^-$) was prepared by published procedures.[1] All solvents were analytical grade.

Syntheses of $\{[Cd_2(L)_2(D/L\text{-}Lm)(H_2O)_2] \bullet 5H_2O\}_n$ (D/L-Cd-MOF)

$CdCl_2 \cdot 5/2H_2O$ (46 mg, 0.020 mmol), $H_2L^+ \cdot Cl^-$ (75 mg, 0.020 mmol), D/L-tartaric acid (45 mg, 0.030 mmol) in mixture of solvents contained water (1.00 mL) and DMAc (2.00 mL), which were sealed in a 25 mL Teflon-lined stainless container and then were heated at 120 °C for 3 days. After the mixture solvents were cooled down to room temperature at 10 °C /min, the colorless block crystals were obtained, then filtered, washed with mixture solvents of DMAc and H_2O, and dried naturally. Yield: 80 % (based on Cd). Anal Calcd for $\{[Cd_2(L)_2(D\text{-}Lm) \cdot (H_2O)_2] \cdot 5H_2O\}_n$ (D-Cd-MOF): C 43.3, N 4.81, H 3.80%. Found: C 44.0, N 4.71, H 3.75%.

The synthesis conditions of L-Cd-MOF crystal are the same as D-Cd-MOF. Yield: 77 % (based on Cd). Anal Calcd for $\{[Cd_2(L)_2(L\text{-}Lm) \cdot (H_2O)_2] \cdot 5H_2O\}_n$ (L-Cd-MOF): C 43.3, N 4.81, H 3.80%. Found: C 43.0, N 4.59, H 3.68%.

The preparation of D-Cd-MOF working electrode

The ITO glass was cleaned with water, ethanol and acetone in turn and dried in the air. 0.0100 g D-Cd-MOF crystal, 0.50 mL methanol and 20.00 μL 5% Nafion were added to the bottle and the mixture solvents were ultrasonic for 30 min. The solution was dispersed to ITO glass by pipettor and let dry overnight at room temperature to obtain the Eu-MOF working electrode.

The preparation of D-Cd-MOF suspension

1 mg crystals of D-Cd-MOF were dispersed in 0.5 M $LiClO_4$ aqueous solution and dispersed uniformly in the solution by ball mill.

Materials Characterization

Single-crystal X-ray diffraction analyses (SCXRD) were performed on a diffractometer with Cu-Kα radiation (Rigaku XtaLAB). Powder X-ray diffraction (PXRD) was recorded at room temperature

in the air using a Rigaku B/Max-RB X-ray diffractometer (Cu, Kα, λ = 1.54178 Å). UV-vis diffuse-reflectance spectra were recorded by a UH4150 spectrophotometer in the range of 1000-200 nm. With $BaSO_4$ as a reference, IR spectra were obtained on an ALPHA II spectrometer using KBr sample plate. Thermogravimetry analysis curves of D/L-Cd-MOF were obtained on an SDT 2960 thermoanalyzer under a nitrogen atmosphere from room temperature to 800 ^{o}C at a heating rate of 10 ^{o}C/min. For X-ray photoelectron spectroscopy (XPS) measurements, an Al-Kα (120 W) X-ray resource was used, which was performed by Axis Supra. Cyclic voltammetry experiments were recorded on an electrochemical analyzer (CHI 660E) using L/D-Cd-MOF film as the working electrode, with a Pt wire as the counter electrode, and a Ag wire as the reference electrode. The electronic absorption spectra of L/D-Cd-MOF suspension were carried out on an AvaSpec-ULS2048 spectroelectrochemical in the voltage range from -0.84 V to -1.26 V, and the voltage was gradually reduced to 0.04 V. The C, H and N elemental analyses were performed on a Perkin-Elmer 240 elemental analyzer.

Table S1. The crystal data and structure refinements of D/L-Cd-MOF.

Compound	**D-Cd-MOF**	**L-Cd-MOF**
CCDC number	2091298	2091299
Empirical formula	$C_{42}H_{44}Cd_2N_4O_{21}$	$C_{42}H_{44}Cd_2N_4O_{21}$
Formula weight	1165.61	1165.63
Temperature / K	293(2)	200.00(10)
Crystal system	monoclinic	monoclinic
Space group	$P2_1$	$P2_1$

***a* / Å**	8.81340(15)	8.74302(7)
***b* / Å**	24.0719(4)	23.97044(18)
***c* / Å**	10.19512(14)	10.19537(8)
***α* / °**	90	90
***β* / °**	90.01	90.06
***γ* / °**	90	90
Volume / Å^3	2162.95(6)	2136.68(3)
Z	2	2
ρ_{calc} g / cm^3	1.790	1.812
μ / mm^{-1}	8.681	8.788
F(000)	1176.0	1176.0
Crystal size / mm^3	0.3 × 0.26 × 0.23	0.041 × 0.033 × 0.03
Radiation	Cu Kα (λ = 1.54184)	Cu Kα (λ = 1.54184)
2Θ range for data collection / °	7.344 to 146.488	7.376 to 140.142
Index ranges	$-10 \leq h \leq 5$, $-28 \leq k \leq 29$, $-11 \leq l \leq 12$	$-10 \leq h \leq 10$, $-29 \leq k \leq 29$, $-12 \leq l \leq 12$
Reflections collected	6188	20167
Independent reflections	5140 [R_{int} = 0.0595, R_{sigma} = 0.0775]	8126 [R_{int} = 0.0274, R_{sigma} = 0.0268]
Data / restraints / parameters	5140/77/558	8126/219/633

Goodness-of-fit on F^2	1.015	1.022
Final R indexes [I >= 2σ (I)]	R_1 = 0.0460, wR_2 = 0.1158	R_1 = 0.0355, wR_2 = 0.1020
Final R indexes [all data]	R_1 = 0.0471, wR_2 = 0.1166	R_1 = 0.0355, wR_2 = 0.1020
Largest diff. peak/hole / e $Å^{-3}$	0.85/-0.86	0.58/-1.25
Flack parameter	0.016(13)	0.005(8)

$R_1 = \sum||F_o|-|F_c|\sum/|F_o|$. $wR_2 = [\sum w(F_o^2 - F_c^2)_2/\sum w(F_o^2)_2]1/2$

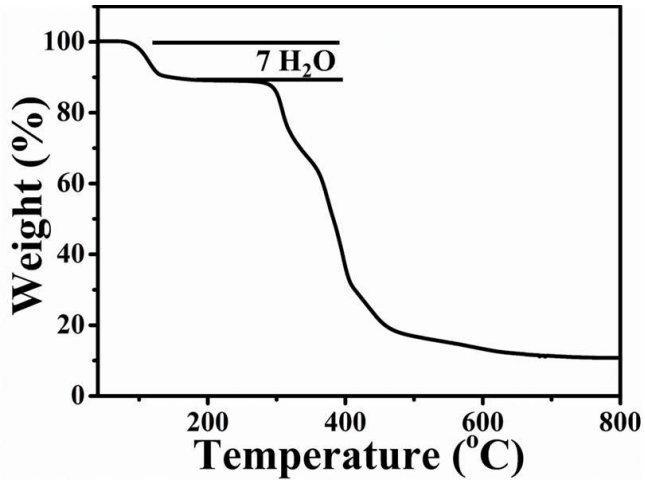

Figure S1. The TGA curves of D-Cd-MOF.

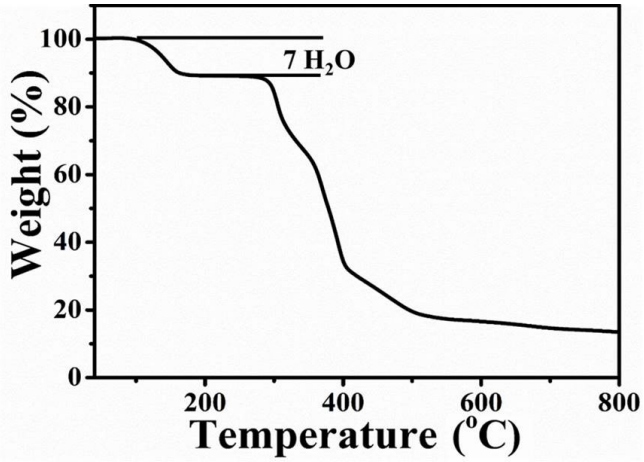

Figure S2. The TGA curves of L-Cd-MOF.

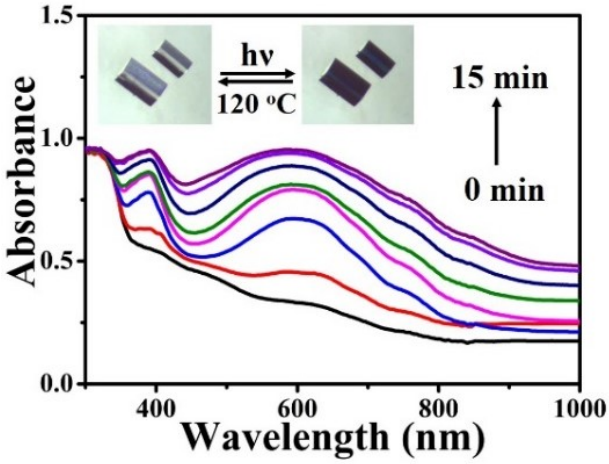

Figure S3. Time-dependent UV−vis adsorption spectra of L-Cd-MOF under UV irradiation. The insert photographs were L-Cd-MOF crystals before and after UV light irradiation.

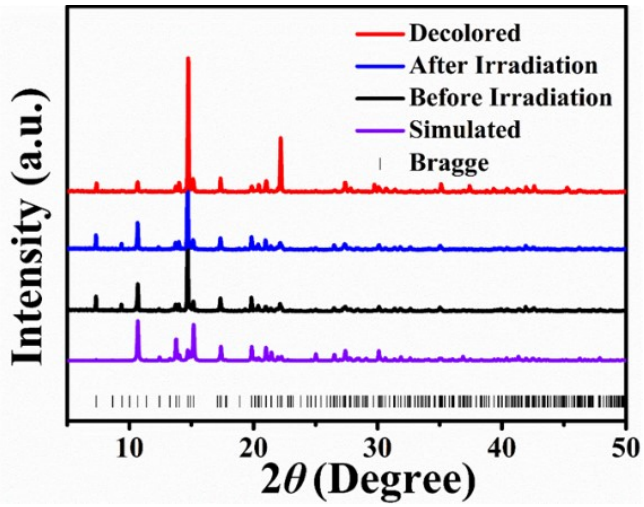

Figure S4. Simulated and experimental PXRD patterns for D-Cd-MOF before irradiation, after irradiation and decolored.

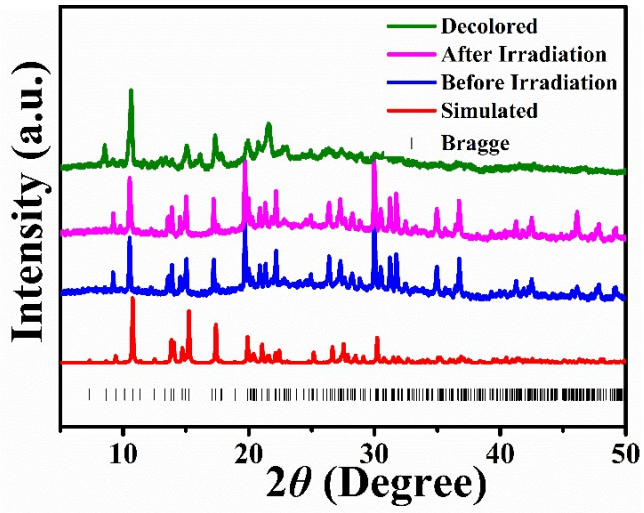

Figure S5. Simulated and experimental PXRD patterns for L-Cd-MOF before irradiation, after irradiation and decolored.

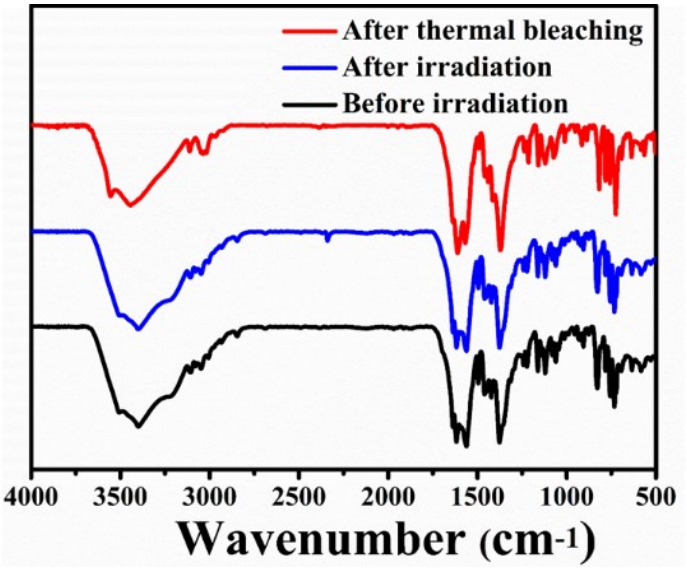

Figure S6. The FT-IR spectra for D-Cd-MOF after thermal bleaching, after irradiation, and before irradiation.

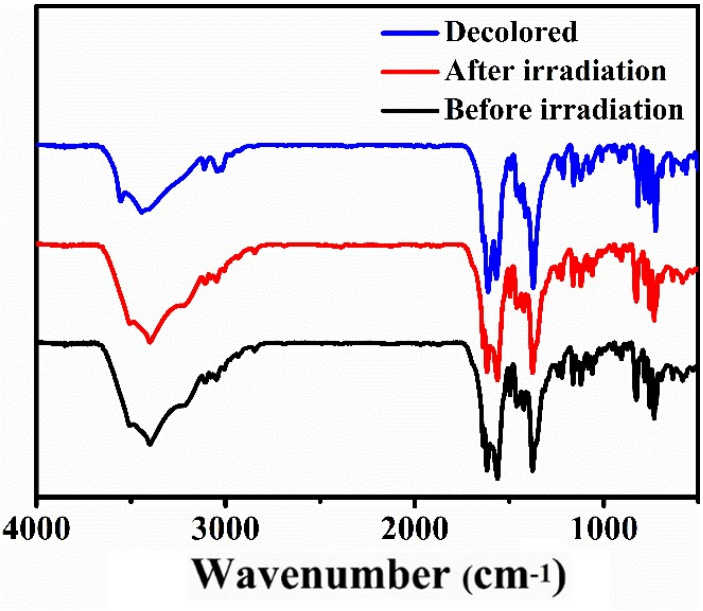

Figure S7. The FT-IR spectra for L-Cd-MOF after thermal bleaching, after irradiation, and before irradiation.

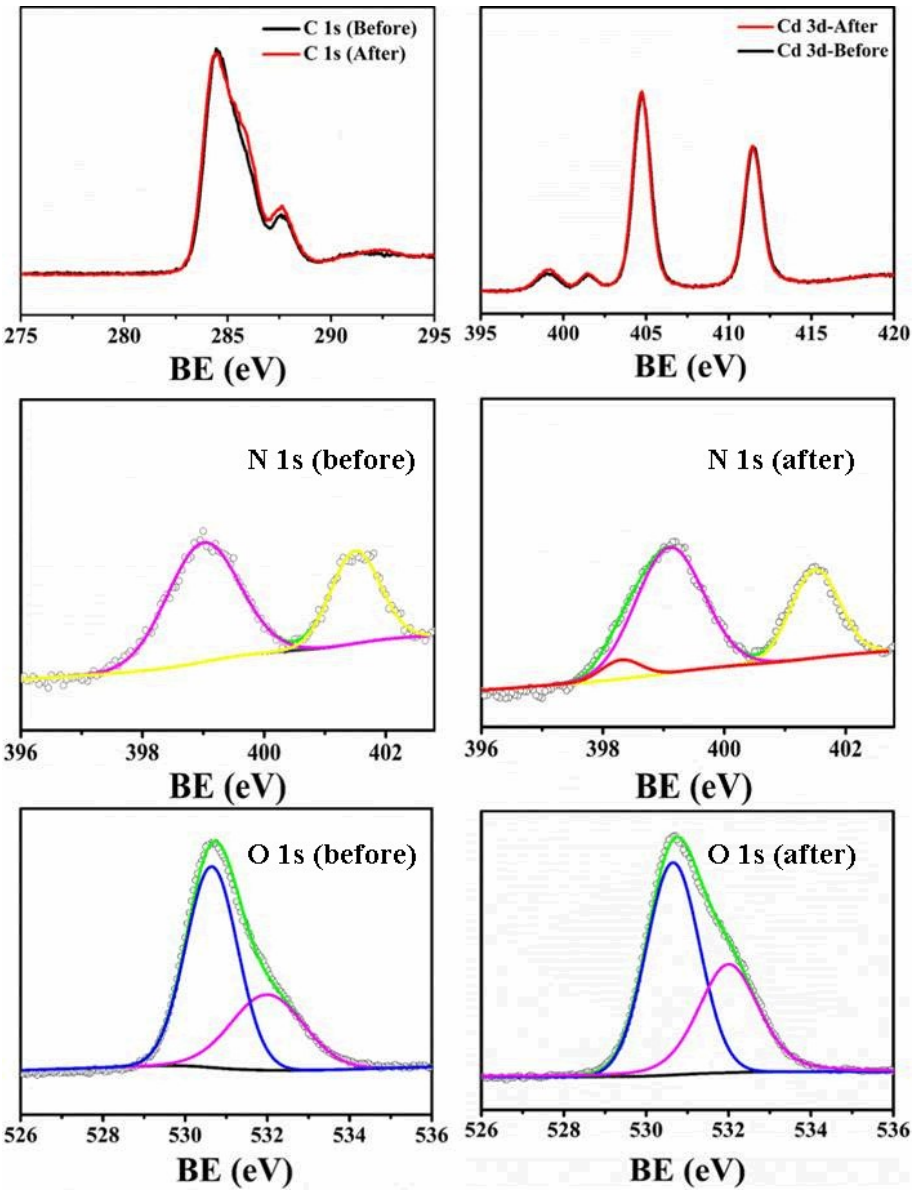

Figure S8. High-resolution XPS spectra of D-Cd-MOF before and after irradiation.

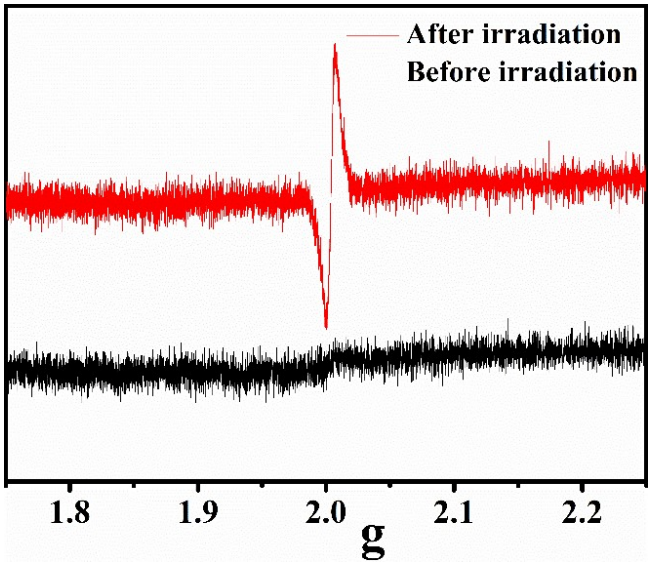

Figure S9. ESR spectra of L-Cd-MOF before irradiation (black line) and after irradiation (red line).

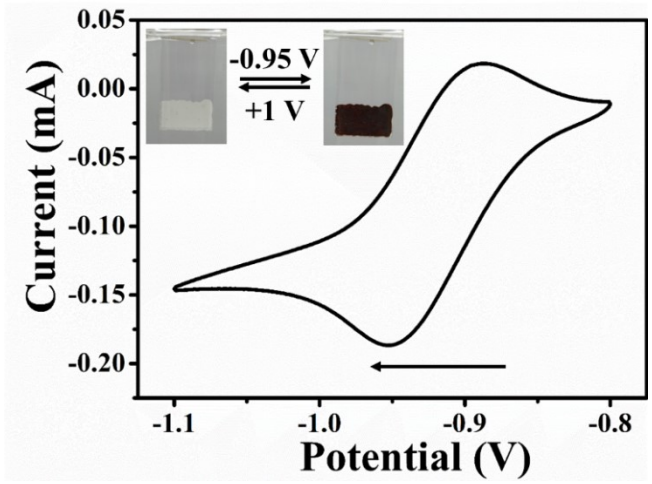

Figure S10. Cyclic voltammogram of L-Cd-MOF measured in 0.1 M $LiClO_4$ solutions via scan voltage from -0.8 V to -1.1 V.

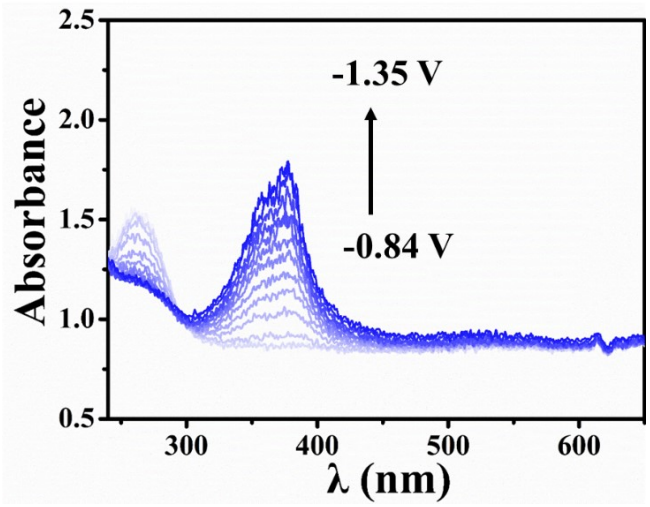

Figure S11. Absorption spectra of L-Cd-MOF suspension upon applying potentials from -0.84 V to -1.35 V.

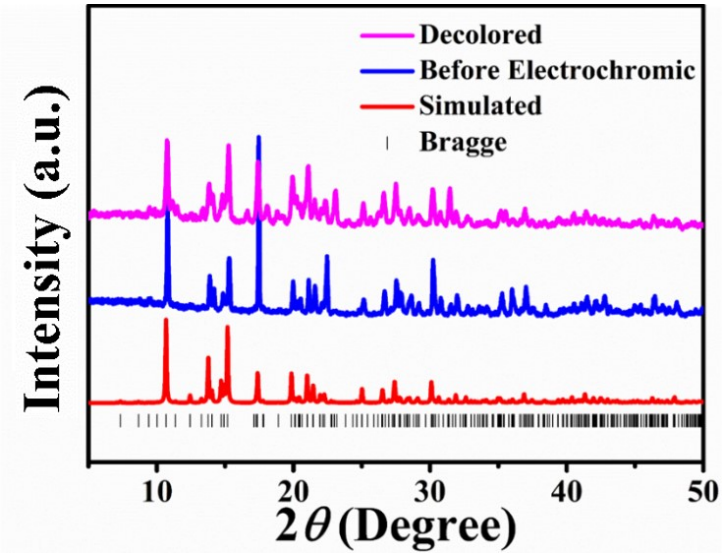

Figure S12. Simulated and experimental PXRD patterns for D-Cd-MOF at decolored and before electrochromic state.

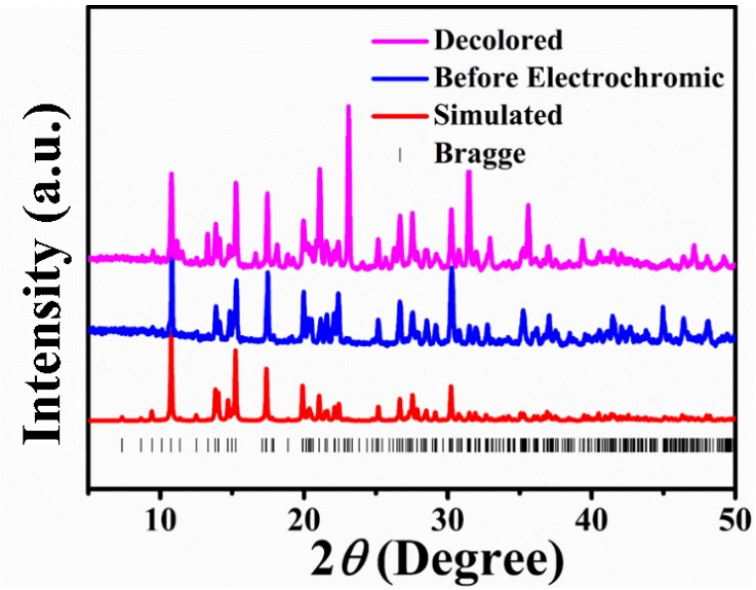

Figure S13. Simulated and experimental PXRD patterns for L-Cd-MOF at decolored and before electrochromic state.

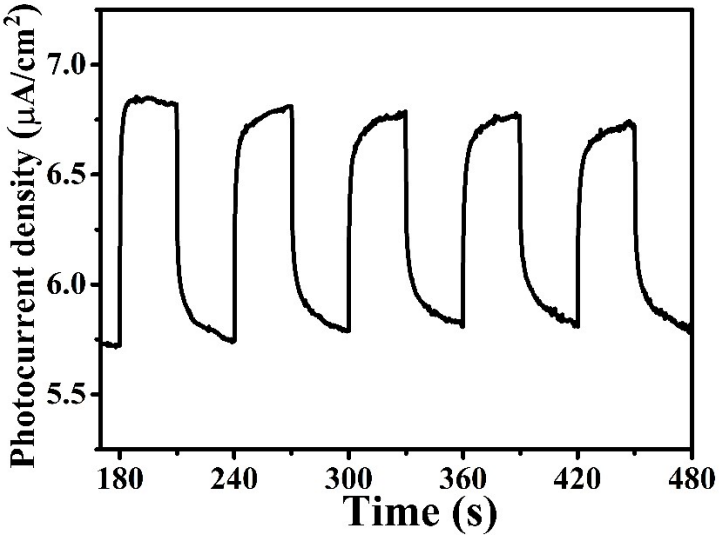

Figure S14. Photocurrent response behaviours for D-Cd-MOF.

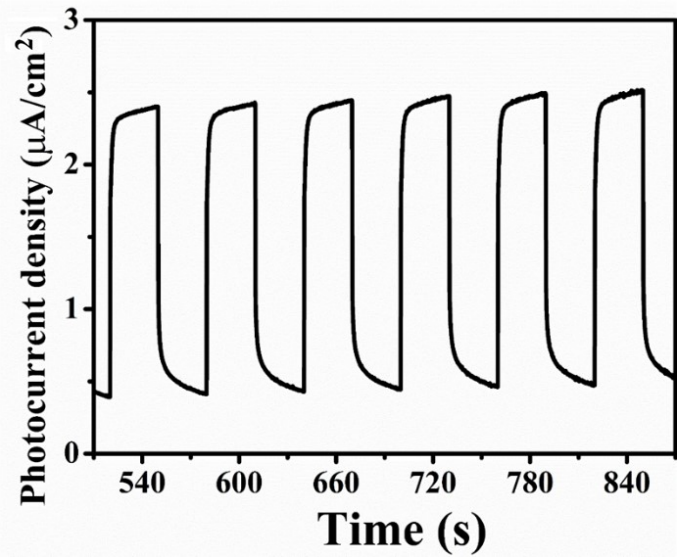

Figure S15. Time-dependent photocurrent density for L-Cd-MOF.

References

1. H. Y. Li, J. Xu, L. K. Li, X. S. Du, F. A. Li, H. Xu, S. Q. Zang, *Cryst. Growth Des.*, 2017, **17**, 6311-6319.